Electron-electron interaction in carbon-coated ferromagnetic nanowires

M. Brands,* A. Carl, O. Posth, and G. Dumpich
Fachbereich Physik, Experimentalphysik, Universität Duisburg-Essen, 47048 Duisburg, Germany
(Received 26 April 2005; revised manuscript received 14 June 2005; published 29 August 2005)

We have investigated the low temperature resistance behavior and the magnetoresistance of single-domain cobalt nanowires of various thicknesses ranging between 5 nm and 32 nm and wire widths ranging down to 32 nm. The nanowires are coated with insulating carbon on three sides to prevent oxidation. Magnetic force microscopy investigations show that nanowires with widths below 800 nm are in a single-domain-like remanence state. The magnetoresistance is negative and is well explained by the anisotropic magnetoresistance (AMR). At low temperatures $T<30$ K a logarithmic resistance increase is observed with decreasing temperature, which is consistently explained as originating from enhanced electron-electron interactions in two dimensions. Quantum corrections due to weak electron localization are not observed which is in contrast to recent theoretical predictions for two-dimensional ferromagnetic systems. However, the results are consistent with our earlier results obtained for platinum-capped and unprotected cobalt nanowires. A reduction of the wire width below about 400 nm yields a crossover behavior from two-dimensional to one-dimensional behavior with respect to the quantum corrections of the resistance.

DOI: 10.1103/PhysRevB.72.085457 PACS number(s): 73.20.Fz, 73.50.−h, 75.47.−m, 75.75.+a

I. INTRODUCTION

Electronic quantum transport phenomena have been intensively investigated during the past 20 years. Prominent examples are persistent currents,[1] nonlocal transport phenomena,[2] and universal conductance fluctuations[3] in mesoscopic metallic systems. Particularly, for nonmagnetic thin films a logarithmic resistance increase towards low temperatures is often observed, which results from either weak electron localization (WEL) and/or enhanced electron-electron interactions (EEI) in two dimensions rather than from the well-known Kondo effect.[4] While WEL effects are due to phase coherent backscattering of noninteracting electrons in the presence of weak disorder,[5] EEI effects arise from a modified screening of the Coulomb interaction of interacting electrons due to diffuse scattering.[6] Both effects may be identified experimentally upon application of an external magnetic field oriented perpendicular to the sample plane. For WEL, rather small magnetic fields of the order of $B_\phi=0.01T$ are already sufficient to (partially) destroy the phase coherence between electron waves on length scales of the order of $L_\phi=(\hbar/4eB_\phi)^{1/2}$. This then leads to a low-field positive or negative magnetoresistance (MR) depending on whether or not spin-orbit interactions have to be taken into account.[7] On the other hand, EEI effects are hardly affected by such small external magnetic fields and a respective MR due to EEI only occurs at larger magnetic fields $B>1$ T (at $T=4.2$ K).[8] As a consequence, investigations of the *slope* of the logarithmic resistance increase versus temperature as a function of the applied perpendicular magnetic field allows one to differentiate between both effects.[9,10]

If a thin metallic wire consists of a *ferromagnetic* material, the magnetization $\vec{M}$, or respectively the magnetic induction inside the sample, will provide an internal magnetic field $\vec{B}$ which already may or may not destroy the phase coherence of the backscattered electron waves due to the vector potential $\vec{A}$. Previous experiments indicated that in ferromagnetic thin films EEI is predominant rather than WEL effects.[11–13] On the other hand, Aharanov-Bohm oscillations of the resistance in FeNi nanowires[14] indicate that interference effects are present.[15] Also, recent theoretical calculations have been discussed controversially.[16–20] In our own recent experiments where we investigated the low temperature resistance behavior of Co nanowires we did not find any evidence for WEL effects.[21] To protect the Co wires against oxidation we covered them with a thin (2 nm) platinum layer. Since it is known that Pt—adjacent to a ferromagnetic layer—can be polarized, the question may arise whether or not the Pt layer influences the transport properties of the Co nanowire.

We have therefore extended our studies towards thin cobalt wires covered by *non*metallic carbon protection layers. Again, the magnetoresistance (MR) of the cobalt wires is found to mainly originate from the anisotropic magnetoresistance (AMR) and, again, we do *not* observe any WEL effects, at least within the accuracy of our measurements. Instead, only EEI effects are found to contribute to the low temperature resistance behavior of the Co wires, similar as in the case of Pt-covered Co wires. In addition, we have reduced the wire width to values as small as 32 nm and we thereby observe a crossover from two-dimensional to one-dimensional behavior with respect to EEI effects. Moreover, magnetic iron, nickel, and chromium nanowires show a similar behavior, which confirms that WEL effects are not observable in ferromagnetic samples.

II. EXPERIMENT

Co wires are fabricated by high-resolution electron beam lithography (HR-EBL) onto Te-doped GaAs substrates with dimensions of $3.9\ \text{mm}\times 3.9\ \text{mm}\times 0.525$ mm, subsequent electron beam evaporation in an UHV chamber with a base pressure of 1×10^{-8} mbar, and lift-off technique. Some of the wires were allowed to develop an oxidation layer on top

(and side walls) after preparation while others are protected *in situ* by a 10-nm-thick layer of amorphous carbon. For this we have designed a particular customized resist profile with a strong undercut and in combination with the high surface mobility of carbon atoms during the evaporation process we succeded in a perfect protection against oxidation not only of the top of the wire but also of both side walls of the nanowire. Moreover, the nanowires have a perfect rectangular cross section with almost no tear-off edges.[22] We use *non*magnetic contact wires as well as *non*magnetic contact pads for the resistance measurements in order not to disturb the magnetic configuration of the wires. Note, that for nanowires covered with an insulating material, the common two-step EBL process will not work. We have therefore developed a three-step EBL process where two thin ($t \approx 5$ nm) platinum wires are fabricated first, which then serve as contact leads. On top of (and across) these leads the cobalt nanowire is prepared, which is subsequently covered *in situ* by an insulating carbon layer. Finally, in a third EBL step, the platinum wires are contacted by gold leads. A more detailed description of this fabrication scheme can be found in Ref. 22.

The typical length of the wires varies between $l=40$ μm and $l=100$ μm and we have systematically varied both the thickness of the wires ranging between $t=5$ nm and $t=32$ nm and the wire widths between $w=32$ nm and $w=5200$ nm. Typical values of the resistance of narrow nanowires are in the kOhm regime. The resistance is measured via an ac-resistance bridge in a ^{4}He bath cryostate within a temperature range between $T \approx 1.4$ K and $T=300$ K. Magnetic fields of up to $B=5$ T can be applied perpendicular to the wire but parallel to the sample plane (transversal, B_y) as well as perpendicular to the wire and perpendicular to the sample plane (perpendicular, B_z). In addition, measurements in the longitudinal geometry [magnetic field and electric current in-plane, directed along the long wire axis (x direction)] are used to characterize the magnetic remanence state of the wires. Only small electrical currents ranging between $I=10$ nA and $I=3$ μA are used in order to minimize heating effects. The achieved measurement resolution is of the order of $\Delta R/R=5\times10^{-7}$.

III. RESULTS AND DISCUSSION

A. Structural properties

Structural investigations were carried out by using a Philips CM12 transmission electron microscope (TEM), for which cobalt thin films and nanowire arrays were additionally fabricated onto NaCl substrates, precoated by a 15-nm-thick layer of amorphous carbon. The morphology of thin films and nanostructured samples is identical as long as the lateral dimensions of nanostructured samples do not reach below 30 nm.[23] The wires are polycrystalline in nature, having an average grain size of $\Phi=7\pm2$ nm. The edge roughness of nanowires is of the order of the grain size. Electron diffraction patterns indicate the predominance of hexagonal closed packed ($\epsilon-$) cobalt with a number of stacking faults.

B. Magnetic properties

For a detailed interpretation of the results of magnetoresistance measurements of single cobalt nanowires, it is indispensable to exactly know the magnetic configuration of the wires, especially within the remanence state. We have therefore carried out magnetic force microscopy (MFM) investigations by using a Digital Instruments D3000 MFM utilizing standard "magnetic etched silicon probe" (MESP) magnetic tips. Figure 1 shows MFM images of two different carbon-covered cobalt nanowires with different width but the same thickness of 20 nm. For each wire, three MFM images were taken, one at each end of the wire and one image at the middle section of each wire. Note that since the typical length of a nanowire is of the order of 50 μm, there is a rather large distance between each of the images. Prior to imaging, both wires were magnetically saturated within a magnetic field of $B=2$ T applied in plane along the long wire axis (longitudinally). The nanowire displayed in the lower part of Fig. 1 has a width of about 400 nm and the MFM image exhibits two distinct poles situated at the wire ends, represented by a spot with dark image contrast on the left side, and a spot with bright image contrast on the right side. At other locations along the wire axis no significant MFM contrast is detected, except for some minor contrast spots which result from morphological contributions, as typically represented by the middle image. In MFM, only the gradient of the stray field is detected, which emerges from the sample, where any attractive interaction between the magnetic tip and the stray field is converted into dark image contrast, while any repulsive interaction is converted into bright image contrast. Thus, the MFM image of the wire as shown in the lower part of Fig. 1 can be interpreted such that this wire consists of a *single-domain-like* remanence state whereby the magnetization is oriented in plane, directed along the long wire axis. The reason for this is a strong magnetic shape anisotropy related to the high aspect ratio, the ratio of length and width of the wire. In contrast, the nanowire with a width of 2.16 μm presented in the upper part of Fig. 1 clearly shows the typical features of an in-plane *multidomainlike* magnetic state, which is obvious from the image contrast, which varies along the whole wire. Note that for the investigated wire thickness of $t=20$ nm, the domain walls are of the Néel type with in-plane magnetization components only. The more prominent spots with bright and dark image contrast located at the wire ends are reminiscent of the single-

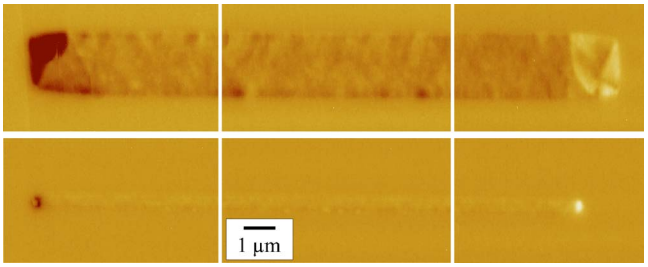

FIG. 1. (Color online) Magnetic force microscopy (MFM) images taken at remanence for two carbon-covered cobalt nanowires of different width but the same thickness of 20 nm. Both wires were magnetically saturated prior to imaging within a magnetic field of $B=2$ T applied longitudinally. While the upper wire ($w=2.16$ μm) is in a multidomainlike magnetic state at remanence, the narrow wire ($w=400$ nm, lower image) is in a single-domain-like state.

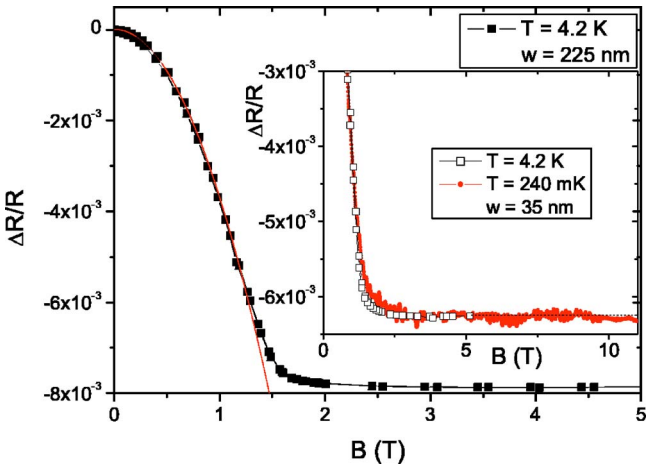

FIG. 2. (Color online) Perpendicular magnetoresistance (MR) of a Co nanowire with width $w=225$ nm covered with a 10 nm carbon layer. The MR continuously decreases until it reaches a saturation value of about –0.8% due to the anisotropic magnetoresistance (AMR). The absolute value of the resistance in a zero magnetic field is $R_0=10395\ \Omega$. The inset shows the perpendicular MR for a carbon-covered cobalt nanowire with a width of 35 nm measured at temperatures of $T=4.2$ K and $T=240$ mK. Both measurements are identical and up to magnetic fields of $B=11$ T; no other contribution other than the AMR effect is observed.

domain state of small wires and they result from the fact that most of the magnetization components are still directed along the wire axis as in the case of narrow wires. A systematic investigation of carbon-covered nanowires with varying width shows that the transition from a multidomainlike remanence state to a single-domain-like magnetic state occurs for wire widths of about 800 nm. This is consistent with former investigations carried out for 30-nm-thick cobalt nanowires covered with 2 nm platinum, which displayed a transition width in between 1 μm and 2 μm for similar wire lengths.[24]

C. Magnetoresistance behavior

The overall resistance behavior of the carbon-covered Co nanowires is metallic, accompanied by a linear temperature dependence of the resistance for temperatures $T>50$ K (not shown here). The residual resistance ratio $\Gamma=R(300\ \mathrm{K})/R(4.2\ \mathrm{K})$ is of the order of $\Gamma\approx1.5$ and the residual resistance of all samples varies between ρ (4.2 K) $=20-30\ \mu\Omega$ cm, which is comparable to earlier results.[25] Applying magnetic fields along the wire axis (longitudinal) the MR is almost constant except for sharp resistance minima which occur at the coercive fields H_c. This behavior can be explained by nucleation and traversal of magnetic domains based on the AMR effect.[24–27] If the magnetic field is applied transversal and in plane to the Co nanowire the resistance strongly decreases in small magnetic fields following a $R\propto B^2$ law, which can be explained by a coherent rotation of the magnetization based on the AMR effect.[29,30] Upon further increasing the field the resistance remains constant.

Figure 2 shows the perpendicular MR behavior of a 20-nm-thick Co nanowire with a length of 200 μm and a width of $w=225$ nm. The inset shows in an enlarged scale the MR of a very narrow Co nanowire (width $w=35$ nm) measured at $T=4.2$ K and $T=240$ mK up to magnetic fields of $B=11$ T. As one can see from Fig. 2 the resistance of both Co nanowires exhibits a continuous decrease up to about $B=1.7$ T which is the saturation field of Co in the hard axis[31] and remains constant upon applying higher magnetic fields. Similar to the transversal case we find that $R(B)$ can be fitted with $\Delta R(B)\propto -B^2$ (see solid line in Fig. 2) as originating from the AMR. A detailed analysis of the $R(B)$ curves yields a magnetic anisotropy constant $K_{eff}=9.51\times10^5\ J/\mathrm{m}^3$ which is 91% of the literature value for the shape anisotropy of cobalt at $T=4.2$ K.[32] Crystalline anisotropy contributions can be neglected since our samples are polycrystalline. This means that the MR behavior reflects a coherent rotation of the magnetization when applying a magnetic field perpendicular to the sample plane. Note that this behavior is independent of the wire width which in turn shows that, independent of whether the remanent state exhibits a multidomain-like or a monodomain-like configuration, the magnetization rotates from in plane to out of plane until it saturates for fields larger than $B_{sat}=1.7$ T. In both the transverse and perpendicular case the resistance decreases in total by about 0.8% which is also typical for the AMR effect.[28,31] Note also that we do not observe any $R\sim B^2$ contribution as resulting from the (classical) Lorentz magnetoresistance (LMR) at high magnetic fields. This appears to be reasonable, since the elastic scattering length l_e of the conduction electrons is of the order of only 7 nm. We also do not observe any contribution from spin-disorder MR which is reasonable, since this contribution is negligible at low temperatures. Thus, the overall MR behavior of cobalt nanowires can be well explained as resulting solely from the AMR effect. Moreover, and this is the most striking feature of the MR, the resistance remains constant, even if the magnetic field strength is increased up to $B=11$ T and for temperatures down to $T=240$ mK as shown in the inset of Fig. 2. This means that we do not find any indication of a negative or positive MR as is expected if WEL effects were present.

D. Temperature dependence

Figure 3 shows the resistance of a 20-nm-thick carbon-covered cobalt nanowire with a width of $w=5.2$ μm as a function of the logarithm of the temperature for various magnetic fields applied perpendicular. As one can see the resistance exhibits a resistance minimum at about $T=9$ K and a logarithmic resistance increase with further decreasing temperature. Upon application of various magnetic fields the resistance (at $T=$const) decreases according to the AMR effect, as discussed above. However, the slope of the logarithmic resistance versus temperature behavior does not change within the whole magnetic field range up to magnetic fields of $B_z=4$ T. In the following, the logarithmic slope of the $R_s(\ln T)$ behavior over one decade of temperature is characterized by

$$\Delta G(10)=G(10\ \mathrm{K})-G(1\ \mathrm{K})=\frac{R_s(1\ \mathrm{K})-R_s(10\ \mathrm{K})}{R_s(10\ \mathrm{K})^2}, \quad (1)$$

where R_s is the sheet resistance. Figure 4 displays the magnetic field dependence of the slope $\Delta G(10)$ as defined in Eq.

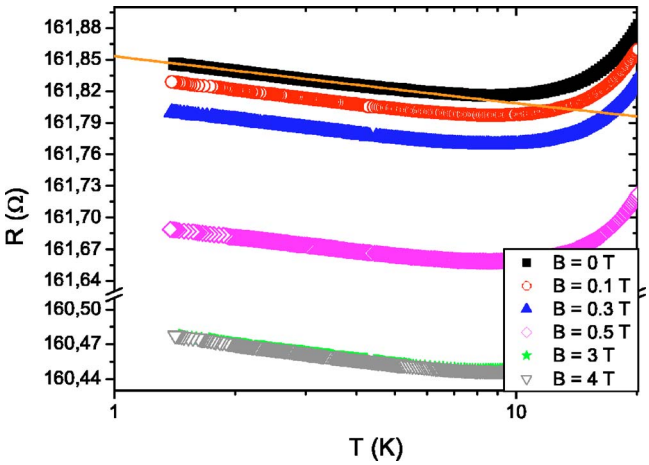

FIG. 3. (Color online) Resistance of a cobalt wire with a thickness of 20 nm and a width of 5.2 μm as a function of the logarithm of the temperature for various magnetic fields applied perpendicular to the substrate plane. While the slope of the different curves remains constant the absolute values of the resistance decrease due to the AMR effect (note the break in the R axis). The full line represents a fit according to the theory for enhanced electron-electron interactions in two dimensions (Refs. 33 and 34).

(2) for two different carbon-covered cobalt wires with a thickness of 20 nm and wire widths of 5.2 μm and 440 nm, respectively. As one can see, we find $\Delta G(10)=2.76\times10^{-5}\square/\Omega\pm1.0\%$ and $\Delta G(10)=3.30\times10^{-5}\square/\Omega\pm2.0\%$, which are independent of the applied magnetic field for both cobalt wires of different widths.

As shown in Fig. 1 and discussed in the previous section (see also Fig. 2) the Co nanowires are in-plane magnetized. Since the demagnetization field H_d is in this case almost zero or $N_{xx}=0$, the internal magnetic induction is $B_i=\mu_0 M_x$ in the remanent state and points in plane along the long wire axis. In this case the vector potential $\vec{A}$ is oriented perpendicular to the current direction and has therefore no influence on the electron wave function according to the Aharanov-Bohm effect. Thus, if WEL effects were present, they should not be destroyed by internal magnetic induction fields since the corresponding magnetic flux does not penetrate any self-intersecting paths of backscattered electron waves. Consequently, one should observe (in the two-dimensional case) a logarithmic resistance increase. Applying a magnetic field perpendicular to the sample plane, the internal magnetic induction equals the externally applied field since the demagnetization factor in the z direction is $N_{zz}=1$. In this case the vector potential $\vec{A}$ is oriented in plane acting on the phase of the electron wave function which consequently should lead to a reduction of WEL effects, if they were present. Then, however, we should expect that the logarithmic slope would change upon application of the (perpendicular) magnetic field. Since we do not observe such a variation of the slope as a function of the magnetic field (Fig. 4), this clearly indicates that WEL effects are obviously not present. Note that the Co wires discussed so far have typical widths of some μm revealing a multidomainlike remanence state as shown in Fig. 1. Due to the strong shape anisotropy, for these wires the magnetization is everywhere oriented within the wire plane, but one might argue that the local variation of the magnetization within Néel-type domain walls would lead to a reduction of WEL effects even in zero magnetic field.[35] However, even for the cobalt wire with a width of 440 nm, which is in a single-domain-like remanent state and can be considered two-dimensional, the respective magnetic field dependence of $\Delta G(10)$ is found to be almost identical as compared to the wire with a width of 5.2 μm (see Fig. 3). Thus, the presence or absence of WEL effects obviously does not depend on the presence of Néel-type domain walls.

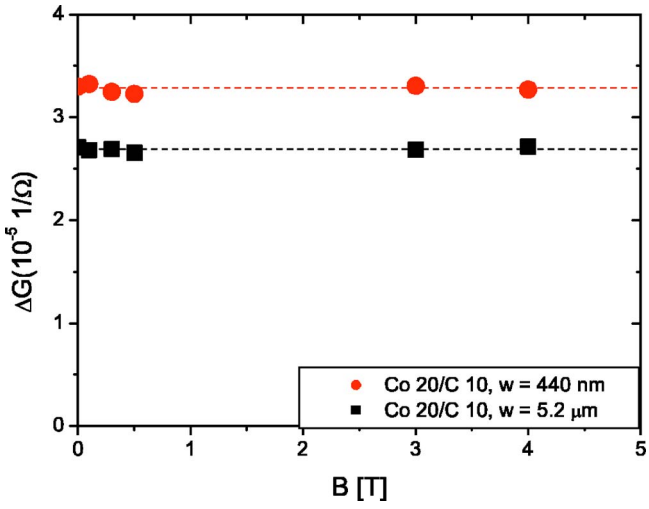

FIG. 4. (Color online) Logarithmic slope of the $R(\ln T)$ behavior, as determined over one decade of temperature, as a function of a magnetic field applied in the z direction for two Co wires with different widths as indicated. No magnetic field dependence of $\Delta G(10)$ is observed, proving that this resistance contribution results from electron-electron interaction effects rather than from WEL effects. The error bar is of the order of the dot size.

Obviously, for our Co wires, the observed logarithmic resistance increase with decreasing temperature is due to enhanced electron-electron interactions. This is also confirmed directly by comparison of our experimental data with theoretical predictions for EEI effects in two-dimensional systems.[33,34] As can be seen from the fit within Fig. 3 (full line), the theoretical result well agrees with our experimental data. The consideration of two dimensionality is justified for the above two wires, since the wire width $w=5200$ nm is much larger than the thermal diffusion length of EEI ($L_T \sim 80$ nm@4.2 K).

It is well known that WEL and EEI effects in one-dimensional systems (where L_T, $L_\phi \gg w,t$) are up to two orders of magnitude larger as compared to the two-dimensional case.[33] This is due to the fact that backscattering effects and also EEI are more effective because of the reduced dimensionality. Thus, if WEL effects would be present, one would expect that they would be more pronounced and more easily observable in one-dimensional samples. We have therefore investigated the resistance behavior of rather narrow cobalt nanowires with widths as small as 32 nm. Figure 5 shows the resistance of a 20-nm-thick carbon-covered cobalt nanowire with a width of $w=40$ nm as a function of the logarithm of the temperature for various magnetic fields applied perpen-

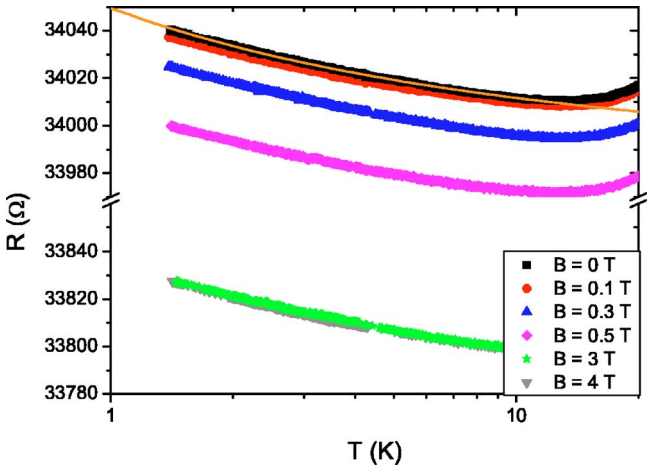

FIG. 5. (Color online) Resistance of a cobalt nanowire with a thickness of 20 nm and a width of 40 nm as a function of the logarithm of the temperature for various magnetic fields applied perpendicular to the substrate plane. The slope of the resistance versus temperature remains constant for various external magnetic fields up to $B=4$ T. The full line represents a fit according to the theory for enhanced electron-electron interactions in one dimension (Refs. 33 and 34).

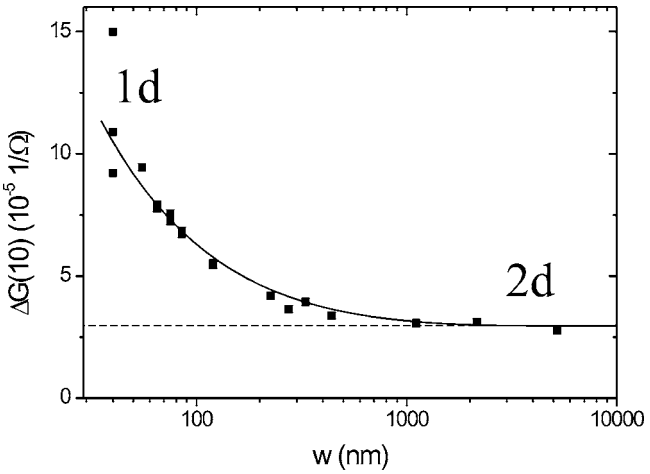

FIG. 6. Slope $\Delta G(10)$ of the resistance increase for a variety of carbon-covered cobalt nanowires as a function of the wire width. The logarithmic scale of the abscissa was chosen for the sake of a better presentation. Starting from the two-dimensional limit of $\Delta G(10) \approx 2.75 \times 10^{-5} \square/\Omega$ values of $\Delta G(10)$ continuously increase with decreasing wire width. The full line is only a guide for the eye.

dicular to the wire plane. Similar to the case of wide cobalt wires the resistance shows a minimum at $T \approx 14$ K and it increases with further decreasing temperature. Again, the slope of the resistance increase does not change upon application of an external magnetic field up to $B=4$ T, whereas the absolute resistance decreases due to the AMR. In contrast to the case of wide Co wires the resistance does not follow a $R(\ln T)$ behavior but it rather shows a $R(T^{-0,5})$ behavior. Indeed, such a behavior is very reminiscent of quantum corrections for the one-dimensional case. It can be best described by a theory designed for the transition regime between one- and two-dimensional cases, which was developed by Neuttiens *et al.*[34] based on theoretical expressions for the true one- and two-dimensional cases derived by Al'tshuler and Aronov,[33]

$$\delta G_{EEI}^{1d-2d}(T) = \frac{\alpha}{\frac{\pi\hbar}{e^2}} \sum_{n=0}^{\infty} \frac{1}{\sqrt{\frac{w^2}{L_T^2} + (n\pi)^2}} - \frac{1}{\sqrt{\frac{w^2}{L_{T_0}^2} + (n\pi)^2}}. \tag{2}$$

Here, $L_T = \sqrt{\hbar D / k_B T}$ is the thermal diffusion length, D the electronic diffusion constant, w the wire width, α a screening constant, and T_0 a reference temperature which, from a mathematical point of view, is needed for the convergence of the row in Eq. (2). For a wire with 40 nm width, the expected resistance behavior (full line in Fig. 5) well agrees with our experimental data. Thus, we may again conclude that in ferromagnetic cobalt nanowires, which are protected with an insulating carbon layer, weak electron localization effects are not observed, independent of the dimensionality of the wire, even down to wire widths of 32 nm. From our measurement resolution we can deduce that magnetic field dependent effects must be smaller than $\Delta G(10) \leqslant 2 \times 10^{-7} \square/\Omega$. Instead, the low temperature resistance behavior can unambiguously be explained as originating from enhanced electron-electron interactions in both one and two dimensions, respectively.

E. Dimensionality

We prepared and investigated a variety of carbon-covered Co nanowires as a function of the wire width to study the two dimensional–one dimensional crossover of the quantum corrections to the resistance based on EEI. Figure 6 shows the resistance increase $\Delta G(10)$ over one decade of the temperature as defined above. The full squares correspond to the experimental data whereas the solid line is only a guide for the eye which illustrates the increase of $\Delta G(10)$ with decreasing wire width. The two-dimensional limit of $\Delta G(10) \approx 2.75 \times 10^{-5} \square/\Omega$ is indicated by a dashed line. Equation (2) also reveals that (i) the increase of the slope of the resistance versus temperature dependence of mesoscopic wires and (ii) the dependence of $\Delta G(10)$ from the wire width are both strongly influenced by the electronic diffusion constant D as well as the screening factor α. Both are used as fitting parameters in Eq. (2). As shown by Neuttiens *et al.*[34] the screening constant is usually determined in the two-dimensional limit and assumed to be independent of the wire width. By using a diffusion constant $D = \frac{1}{3} v_F l_e = 3.5 \times 10^{-3}$ m^2/s where $v_F = 1.5 \times 10^6$ m/s is the Fermi velocity of cobalt and $l_e = 7$ nm the elastic mean free path, we obtain an average value of $\alpha = 0.95$ for the screening constant in the two-dimensional limit. This value of α is in good agreement with $\alpha = 1-1.5$ found by Neuttiens *et al.* for thin gold films. Since the screening constant α is fixed, the only remaining fitting parameter is the electronic diffusion constant D, which is plotted in Fig. 7 as a function of the wire width. We would like to emphasize that, since we have fixed the screening constant α by calculating D in the two-

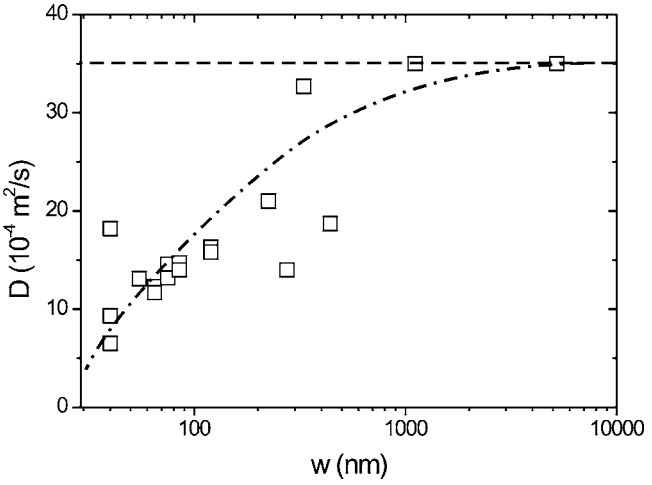

FIG. 7. Electronic diffusion constant D as a function of the wire width as obtained from a fit of Eq. (2) to the resistance versus temperature. In the two-dimensional limit D is given by $D=\frac{1}{3}v_F l_e = 3.5\times10^{-3}$ m^2/s where $v_F=1.5\times10^6$ m/s is the Fermi velocity of cobalt and $l_e=7$ nm the elastic mean free path (dashed line). The dotted line is a guide for the eye and indicates the decrease of D with decreasing wire width w.

dimensional limit, for smaller wire widths, only the *dependence* of D on the wire width is a relevant result, whereas absolute values of D have to be treated with some caution. Nevertheless, values of D are reasonable, and they decrease from $D=3.5\times10^{-3}$ m^2/s in the two-dimensional limit to $D\approx8.0\times10^{-4}$ m^2/s in the one-dimensional limit (dotted line), which can likely be explained by an increasing amount of surface and boundary scattering within the narrow nanowires, which in turn considerably reduces the effective mean free path l_e.

F. Variation of thickness and cap-layer

To further confirm our results, i.e., that EEI effects are dominant rather than WEL effects, we checked whether or not protection layers, material parameters, and the wire thickness influence these findings which is shown in Table I. Cobalt wires without any protection develop an insulating antiferromagnetic CoO layer on top of the cobalt wire. For cobalt thicknesses ranging between 10 nm and 32 nm they exhibit an AMR effect, similar to protected cobalt wires. All cobalt wires investigated—including platinum-capped and unprotected cobalt wires with $w\approx2$ μm of our earlier investigation[21]—show a logarithmic resistance increase to low temperatures which is independent of the magnetic field strength (similar to what is shown in Fig. 4). Nevertheless, from Table I some additional tendencies may be deduced: (i) The sheet resistance R_s increases with decreasing wire thickness due to the smaller wire cross section and the increasing amount of surface scattering. (ii) Unprotected cobalt wires exhibit a rather high resistivity since their effective cross section is diminished due to surface oxidation effects.[25] (iii) A better shielding against oxidation is obviously provided by the carbon cap layer. The AMR effect decreases in magnitude with decreasing wire thickness, but at least to a certain extent this decrease can be hindered for very thin wires by a protection layer of carbon. (iv) Independent of both the wire thickness and the material used as a protective layer, all the Co wires exhibit almost the same magnitude of $\Delta G(10) = (2.85\pm0.4)\times10^{-5}\square/\Omega$. Note that only the results of Co wires in the two-dimensional limit are presented in Table I for the sake of comparability.

TABLE I. Sheet resistance R_s at 4.2 K, AMR effect at 4.2 K (in %), and slope of the logarithmic resistance increase $\Delta G(10)$ for various (quasi-two-dimensional) cobalt nanowires with thicknesses given in nm.

Sample one only	R_s(4.2 K) $\left(\frac{\Omega}{\square}\right)$	AMR (4.2 K) (%)	$\Delta G(10)$ 10^{-5} $\left(\frac{\square}{\Omega}\right)$
Co20	17.9	0.59	2.75±0.21
Co32	8.2	0.78	3.21±0.40
Co05 Pt2	187.9	0.09	3.25±0.08
Co10 Pt2	45.0	0.25	3.05±0.40
Co20 Pt2	7.0	1.06	2.47±0.25
Co30 Pt2	5.7	1.02	2.70±0.34
Co05 Si8	121.3	0.59	3.10±0.15
Co04 C10	190.4	0.08	3.21±0.02
Co07 C10	64.5	0.21	3.19±0.03
Co10 C10	24.2	0.46	2.77±0.03
Co20 C10	10.4	0.84	2.99±0.03
Co30 C10	5.76	0.85	2.87±0.05

G. Material variation

The saturation magnetization of a magnetic nanowire is an important parameter in theoretical calculations of quantum transport effects in ferromagnets.[18,36] We have therefore also varied the saturation magnetization by using different ferromagnetic and antiferromagnetic materials. Figure 8 shows the temperature dependence of the resistance of an iron wire for six magnetic fields up to $B=4$ T applied perpendicular to the sample plane. The shown behavior is exemplary for all nanowires made of nickel and iron. As for the cobalt wires a logarithmic resistance increase to low temperatures is observed which does not depend on the applied field. The absolute resistance decrease is due to AMR. The sole difference in the temperature-dependent resistance curves of nickel, cobalt, and iron nanowires is the position of the resistance minimum. Nickel nanowires have the smallest sheet resistance resulting in the smallest relative resistance increase (though the slope is still of the order of $\Delta G(10) = 2.85\times10^{-5}\square/\Omega$) and therefore the resistance minimum can be observed at $T\approx2.5$ K which makes quantitative investigations increasingly difficult. This is also confirmed from the magnetoresistance investigations of these nanowires (not shown here).

Antiferromagnetic chromium nanowires are special with regard to quantum transport phenomena in magnetic materi-

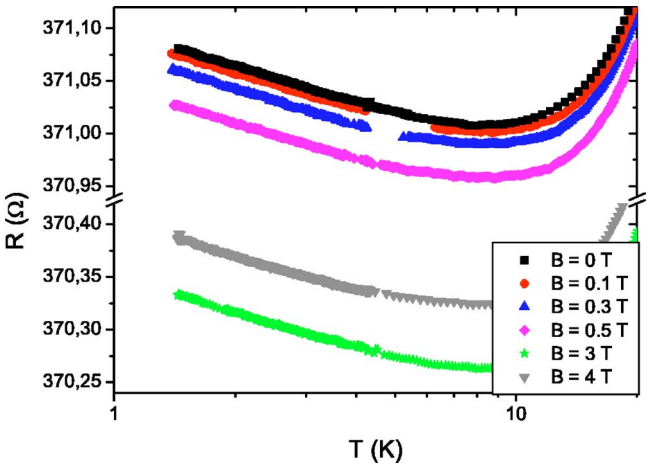

FIG. 8. (Color online) Resistance of an iron nanowire with a thickness of 30 nm and a width of 2.16 μm as a function of the logarithm of the temperature for various magnetic fields applied perpendicular to the sample plane. The slope of the curves remains constant while the absolute resistance decreases due to AMR.

als since ideally their average internal magnetization is zero. However, due to the polycrystalline nature of the samples the local magnetization on an atomic scale may be nonzero. Indeed, the MR of chromium nanowires is typically found to be *very* small ($\Delta R/R < 10^{-5}$). On the other hand, the temperature dependence of the resistance remarkably resembles the behavior as shown above for cobalt, iron, and nickel wires, where we find a logarithmic resistance increase of the order of $\Delta G(10) = 3.49 \times 10^{-5} \square/\Omega$ which is also independent of the applied magnetic field.

IV. CONCLUSION

In conclusion, ferromagnetic nanowires with homogeneous in-plane magnetization which are protected by a thin carbon layer exhibit a logarithmic resistance increase at low temperatures that is independent of an applied perpendicular magnetic field within the accuracy of our measurements. In addition, for cobalt nanowires with various thicknesses ranging between 5 nm and 32 nm, the slope $\Delta G(10) = (2.85 \pm 0.4) \times 10^{-5} \square/\Omega$ of the logarithmic resistance increase is found to be independent of the material used as a protection layer as long as the Co wires are in the two-dimensional limit. From the absence of any field dependence of $\Delta G(10)$ we conclude that weak localization effects are not present in contrast to recent theoretical predictions for two-dimensional ferromagnetic systems. Instead, the experimentally observed resistance increase agrees well with theoretical values for enhanced electron-electron interactions in two dimensions. A reduction of the wire width yields a crossover from two-dimensional to one-dimensional behavior, which is accompanied by an increase in $\Delta G(10)$ and a decrease in the electronic diffusion constant D.

ACKNOWLEDGMENTS

This work is supported by the Deutsche Forschungsgemeinschaft within SFB 491. The authors are grateful to T. Müller and A. Lorke for the resistance measurements at low temperatures and in high magnetic fields. The authors thank C. Hassel for providing the MFM images.

*Electronic address: mario@ttphysik.uni-duisburg.de

[1] M. Büttiker, Y. Imry, and R. Landauer, Phys. Lett. A **96**, 365 (1985).
[2] W. J. Skocpol, P. M. Mankiewich, R. E. Howard, L. D. Jackel, D. M. Tennant, and A. D. Stone, Phys. Rev. Lett. **56**, 2865 (1986).
[3] C. P. Umbach, S. Washburn, R. B. Laibowitz, and R. A. Webb, Phys. Rev. B **30**, 4048 (1984).
[4] J. Kondo, Solid State Phys. **23**, 184 (1969).
[5] E. Abrahams, P. W. Anderson, D. C. Licciardello, and T. V. Ramakrishnan, Phys. Rev. Lett. **42**, 673 (1979).
[6] B. L. Altshuler, A. G. Aronov, and P. A. Lee, Phys. Rev. Lett. **44**, 1288 (1980).
[7] S. Hikami, A. I. Larkin, and Y. Nagaoka, Prog. Theor. Phys. **63**, 707 (1980).
[8] B. L. Altshuler and A. G. Aronov, in *Localization and Electron-Electron-Interactions in Disordered Systems*, edited by A. L. Efros and M. Pollak (North-Holland, Amsterdam, 1985).
[9] S. Friedrichowski and G. Dumpich, Phys. Rev. B **58**, 9689 (1998).
[10] A. Carl, G. Dumpich, and D. Hallfarth, Phys. Rev. B **39**, 3015 (1989).
[11] M. Rubinstein, F. J. Rachford, W. W. Fuller, and G. A. Prinz, Phys. Rev. B **37**, 8689 (1988).
[12] F. G. Aliev, E. Kunnen, K. Temst, K. Mae, G. Verbanck, J. Barnas, V. V. Moshchalkov, and Y. Bruynseraede, Phys. Rev. Lett. **78**, 134 (1997).
[13] T. Ono, Y. Ooka, S. Kasai, H. Mijayima, K. Mibu, and T. Shinjo, J. Magn. Magn. Mater. **226–230**, 1831 (2001).
[14] S. Kasai, T. Niiyama, E. Saitoh, and H. Miyayima, Appl. Phys. Lett. **81**, 316 (2002).
[15] M. Aprili, J. Lesueur, L. Dumoulin, and J. P. Nédellec, Solid State Commun. **102**, 41 (1997).
[16] G. Tatara, H. Kohno, E. Bonet, and B. Barbara, Phys. Rev. B **69**, 054420 (2004).
[17] G. Tatara and H. Fukuyama, Phys. Rev. Lett. **78**, 3773 (1997).
[18] V. K. Dugaev, P. Bruno, and J. Barnas, Phys. Rev. B **64**, 144423 (2001).
[19] A. Singh and E. Fradkin, Phys. Rev. B **35**, 6894 (1987).
[20] T. R. Kirkpatrick and D. Belitz, Phys. Rev. B **62**, 952 (2000).
[21] M. Brands, A. Carl, and G. Dumpich, Europhys. Lett. **68**, 268 (2004).
[22] M. Brands, O. Posth, and G. Dumpich, Superlattices Microstruct. **37**, 380 (2005).
[23] B. Stahlmecke, diploma thesis, University Duisburg-Essen, 2002.
[24] B. Leven and G. Dumpich, Phys. Rev. B **71**, 064411 (2005).
[25] B. Hausmanns, T. P. Krome, and G. Dumpich, J. Appl. Phys. **93**, 1 (2003).
[26] W. Wernsdorfer, K. Hasselbach, A. Benoit, B. Barbara, B. Dou-

din, J. Meier, J.-Ph. Ansermet, and D. Mailly, Phys. Rev. B **55**, 11552 (1997).
[27] S. J. Blundell, C. Shearwood, M. Gester, M. J. Baird, J. A. C. Bland, and H. Ahmed, J. Magn. Magn. Mater. **135**, L17 (1994).
[28] R. McGuire and R. I. Potter, IEEE Trans. Magn. **11**, 1018 (1975).
[29] S. Tumanski, *Thin film magnetoresistive sensors* (Institute of Physics, London, 2001).
[30] M. Brands and G. Dumpich, J. Appl. Phys. **98**, 014309 (2005).
[31] B. D. Cullity, *Introduction to Magnetic Materials* (Addison-Wesley, Reading, Mass., 1972).
[32] P. M. Paulus, F. Luis, M. Krll, G. Schmid, and L. J. de Jongh, J. Magn. Magn. Mater. **224**, 180 (2001).
[33] B. L. Al'tshuler, A. G. Aronov, M. E. Gershenson, and Yu. V. Sharvin, Sov. Sci. Rev., Sect. A **9**, 223 (1987).
[34] G. Neuttiens, J. Eom, C. Strunk, V. Chandrasekhar, C. van Haesendonck, and Y. Bruynseraede, Europhys. Lett. **34**, 617 (1996).
[35] G. Tatara, Int. J. Mod. Phys. B **15**, 321 (2001).
[36] S. Sil (private communication).